Characteristics of a Steel/Clay Model System Under Repository Conditions

Margit Fabian*, Istvan Tolnai*, Otto Czompoly*, Janos Osan*, Elod Laszlo Aradi†

*Centre for Energy Research, Konkoly Thege st 29-33, 1121 Budapest, Hungary, fabian.margit@ek-cer.hu
†Eotvos Lorand University, Pazmany Peter stny 1/A, 1117 Budapest, Hungary

INTRODUCTION

All states that engage in any kind of nuclear application must consider the management of radioactive waste and make sure it is handled in a safe manner regarding the level of radioactivity and complying with national/international regulations. There is a broad consensus that the preferred method of ensuring long term safety for high level radioactive waste (HLW) is isolation in a deep geological repository (DGR), which will provide passive multibarrier isolation of radioactive materials. The vitrified HLW form in a steel canister is specifically designed for long term durability in storage and disposal [1,2]. The requirements for container lifetime and integrity depend on the DGR concept and the chosen geological medium [3].

The focus is on two contacting materials to obtain information on the geochemical evolution close to an interface in terms of chemical variables and alteration in solid phase composition at a detailed small scale.

The interface between carbon steel and clay is a key issue in the design of a disposal cell for vitrified HLW in argillaceous rock formations for the Hungarian national waste disposal program. The design relies on steel-containers (S235JR) containing the HLW encased in a prefabricated cylindrical clay buffer material. The clay is originated from the Boda Claystone Formation (BCF), the host rock considered for the final disposal program in Hungary [4,5]. The pH must be kept at high values during the thermal phase, and for a much longer period after, to keep the carbon steel container passivated for limiting corrosion and ultimately to prevent radionuclide release. The aim of the planned study is to gain information on chemical-physical alterations of the steel/clay interface, for different environmental conditions (temperature, groundwater) using different characterization methods.

II. EXPERIMENTAL DETAILS

II.1. Designs of the experiment

The design of the experiment and the selected parameters, the BCF and the synthetic porewater, are based on the following considerations.

Transport processes are anticipated to remain diffusion-dominated over geologic time frames (hundreds of thousands to millions of years): BCF has a self-healing capacity potential, the weak sensitivity of hydraulic conductivity to changes in loading, there are thick topset beds over the potential disposal zone and the uplift of W-Mecsek is low, so that no major changes in hydraulic gradient are expected, porosity and hydraulic conductivity of the intact rock matrix is very low, a very small amount of swelling clays is fundamentally influencing rock behavior. The flow of free water is limited as well by the size of capillaries. Mostly diffusion processes take place inside the rock even on the level of fractures [4].

Geochemical stability of the groundwater-porewater system over geologic time frames: the lack of organic material and pyrite helps to maintain the long-term geochemical stability of the formation, intensive oxidation processes influencing the rock's mechanical status considerably are not expected to occur within the lifetime of the repository, due to the burial (thermal) history of BCF, the possible impact of heat production of HLW's (e.g. alteration of clay minerals, thermal softening) will be rather limited.

Geomechanical stability of the formations to natural perturbations: the potential disposal zone is protected from the natural perturbations by the thick topset beds.

II.2. Materials and conditions

The experimental set-up was prepared in triplicate as shown in Fig. 1. For each system two Teflon containers are built, to ensure the saturation during the experiments: an external Teflon container: height: 160 mm, diameter: 90 mm and an internal Teflon container: h: 100 mm, d: 50 mm.

The inside is composed by a steel container made of untreated S235JR carbon steel (C-steel) (≤0.17C, ≤0.3Si, ≤1.4Mn, 0.035P, 0.035S, ≤0.55Cu, ≤0.012N (wt.%)), with h: 45 mm and d: 20.64 mm.

The used clayrock from BCF has the following parameters: porosity (%): min: 0.6-max: 1.4; hydraulic conductivity (m/s): 1.0×10^{-15}; solid density (kg/m^3): 2683.23; mineral fraction (wt.%): analcime (13), calcite (12), dolomite (2), quartz (9), Na-plagioclase (11), K-feldspar (4), hematite (6), chlorite (5), muscovite/illite (29), illite/smectite (7); cation exchange capacity (meq/100g): min: 11.2, best estimate: 12, max: 16.2.

The initial water phase considered in the experiment is a synthetic BCF porewater (SBPW) with the following composition (mol/L): Na^+: 1.7×10^{-2}, Ca^{2+}: 3.1×10^{-3}, Mg^{2+}: 2.3×10^{-3}, K^+: 1.8×10^{-4}, Sr^{2+}: 1.5×10^{-5} Cl^-: 2.3×10^{-2}, HCO^{3-}:

6.1×10^{-4}, SO_4^{2-}: 1.9×10^{-3} pH: 8.1, Eh= -300 ± 10 mV (measured at RT) [5].

After filled with the synthetic porewater, all three systems were closed. The clay was kept fully saturated. During the experiment, a constant temperature of 80±2 °C was imposed. The corrosion potential was monitored using a Pt reference electrode. After 3, 7 and 12 months one experimental setup was opened for post-mortem characterization (hereafter referred as CSC-3M, CSC-7M, CSC-12M respectively (CSC as C-steel-clay)).

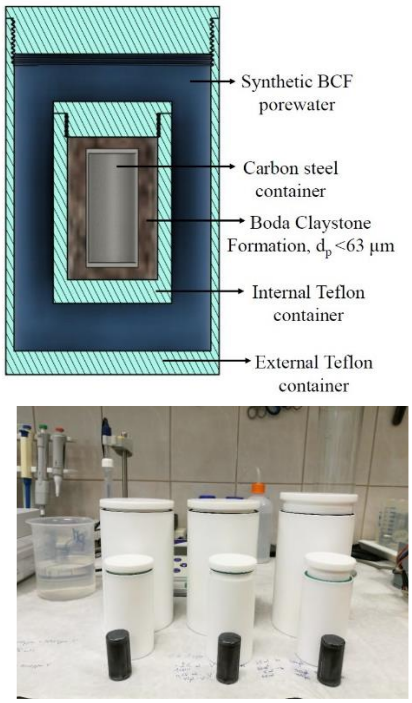

Fig. 1. Cross-section view of one experimental setup indicating different materials (top) and a photograph showing the parts of the experimental setup in triplicate (bottom).

When retrieved, after 3, 7 and 12 months, the C-steel containers were covered with adhering clay making direct characterization of steel surface difficult. The corrosion interfaces were thus investigated on cross-sections.

III. RESULTS

The corrosion products formed on the C-steel-clay interfaces in an anoxic environment on constant 80°C temperature - on the laboratory conditions -, were characterized using different techniques such as SEM/EDX analysis and micro-Raman (is used like µRaman). Changes of cation/anion concentrations in the surrounding synthetic porewater were measured by ICP-OES and IC.

III.1. Corrosion potential

Many clay environments lead to low uniform corrosion rates (less than 10 µm/yr), i.e., anoxic clay environments generally result in a uniform development of corrosion states with low corrosion rates thanks to the formation of protective corrosion products (oxides, carbonates) [6]. The results on the relationship of corrosion potential and months of exposure for CSC samples is illustrated in Fig 2. It is showed that the evolution of corrosion potential measured on the first two C-steel/clay setup (3M, 7M) randomly fluctuate throughout the first and last stage of experiments. It is assumed that an increase in corrosion potential indicates the formation of a passive layer, with a sudden drop indicating the loss of this film layer. This fluctuation indicates local corrosion processes.

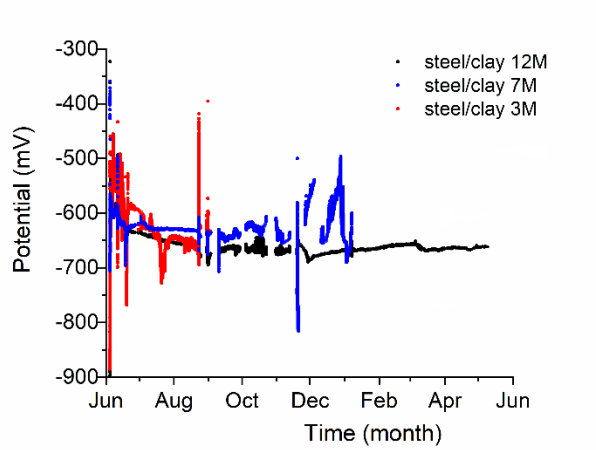

Fig. 2. Corrosion potentials for CSC-3M (red), CSC-7M (blue) and CSC-12M (black).

A decreasing corrosion potential with the time on the CSC-12M sample can be observed after the corrosion is initiated. After that equilibrium was reached, the potential assumed a constant value with a small rise indicating film repassivation, which is remarkable for the CSC-12M sample. Negative potential has been detected throughout the experiments, which is generally considered a higher probability of C-steel corrosion.

III.2. SEM/EDX measurements and results

With scanning electron microscopy/energy dispersive X-ray spectroscopy (SEM/EDX) investigations we focused on the composition and nature of alteration products formed on the steel and within the clay. After reaction times (3, 7, 12 months) on the polished C-steel cylinder SEM/EDX measurements were performed (20 kV, 1.6 nA) using a Thermo Scientific Scios2 dual beam microscope, Oxford X-max^n 20 SDD EDX. On each of the three samples the formation of 30-40 µm long Fe-oxide ingrowths were detected. Figure 3 presents SEM images of the C-steel/clay interfaces after 3, 7, 12 months experimental time. Tables I,

II and III shows SEM-EDX analyses for minerals at the corrosion interfaces of CSC-3M, CSC-7M and CSC-12M samples, based on the marked points on Fig. 3a, Fig. 3b and Fig. 3c.

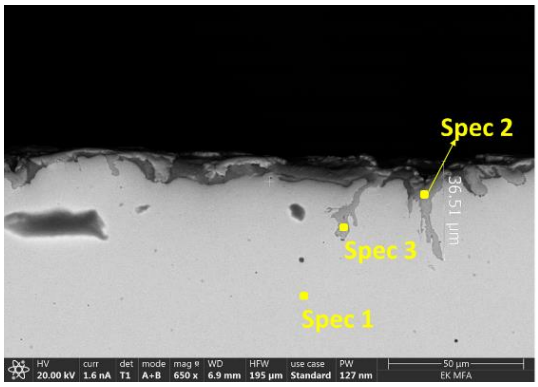

Fig. 3a. SEM micrograph showing micro-cracks initiated on steel exposed for 3 months in a saturated clay.

TABLE I. SEM-EDX analyses for minerals at the corrosion interface of CSC-3M sample (based on the Fig. 3a.).

Spectrum Label	Spec 1 (steel)	Spec 2 (corr. prod)	Spec 3 (corr. prod)
O		48.00	52.64
Si	0.44		
Mn	0.66	0.39	0.26
Fe	98.91	51.61	47.10
Total (at %)	100.00	100.00	100.00

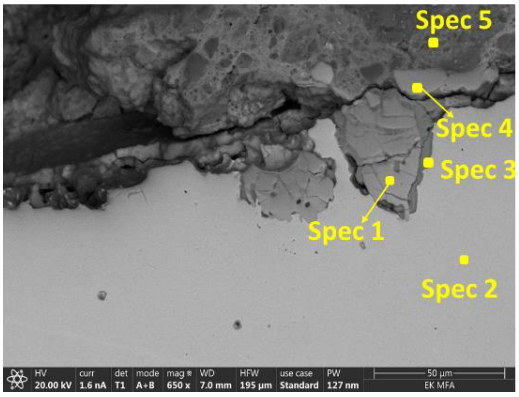

Fig. 3b. SEM micrograph on the C-steel-clay interface after 7 months.

TABLE II. SEM-EDX analyses for minerals at the corrosion interface of CSC-7M sample (based on the Fig. 3b.).

Spec. Label	Spec 1	Spec 2	Spec 3	Spec 4	Spec 5 (clay)
	(corr. prod)	(C-steel)	(corr. prod)	(corr. prod)	
O	48.04		64.90	61.42	67.07
Na					0.64
Mg					2.47
Al					4.11
Si		0.36	0.38	1.49	9.82
K					0.64
Ca					0.78
Cr	0.13			0.52	
Mn	1.08	0.65	0.53	0.88	
Fe	50.74	98.99	34.18	35.68	14.47
Total (at %)	100.00	100.00	100.00	100.00	100.00

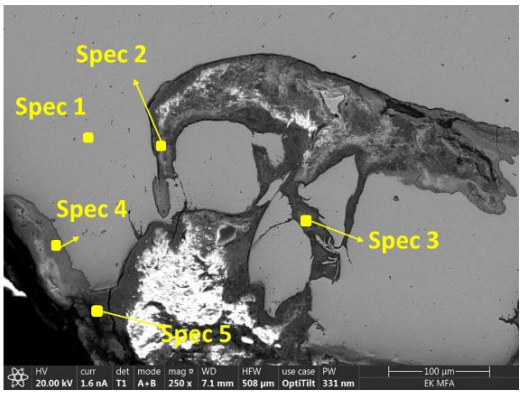

Fig. 3c. SEM micrograph on the C-steel-clay interface after 12 months.

TABLE III. SEM-EDX analyses for minerals at the corrosion interface of CSC-12M sample (based on the Fig. 3c.).

Spec. Label	Spec 1 (C-steel)	Spec 2 (clay)	Spec 3 (clay)	Spec 4 (corr. prod)	Spec 5 (clay)
C	6.51	6.11	4.38	5.76	8.79
O		59.35	58.90	47.08	56.87
Na		1.12	1.35		1.45
Mg		1.76	1.82		1.45
Al		5.46	6.63		4.24
Si	0.38	11.50	15.35	0.32	11.23
K		1.56	1.55		
Ca		1.40	0.78		6.50
Ti		0.09	0.15		0.07
Cl				1.05	0.04
Mn		0.64	0.98	0.32	
Fe	93.11	11.67	9.09	44.27	8.03
Total (at %)	100.00	100.00	100.00	100.00	100.00

The SEM results showed that even in a short term (3M) appeared micro-cracks which can initiate changes of the carbon steel surface (Fig. 3a.). However, these ingrowths

remained relatively short and did not exceed 100 µm in length (Fig. 3b,c).

III.3. µRaman spectroscopy and results

According to the results of the SEM/EDX, the corrosion process has an impact on the steel-clay interfaces. To identify the corrosion products micro-Raman investigations were performed.

The analyses were carried out using a HORIBA JobinYvon LabRAM HR 800 Raman microspectrometer. A frequency doubled Nd-YAG green laser with a 532 nm excitation wavelength was used to illuminate the samples, displaying ~0.2 mW on the sample surface. An OLYMPUS 50× (N.A. = 0.6) and 100× (N.A. = 0.9) objective was used to focus the laser. For Raman mapping 100 µm confocal hole, 600 grooves/mm optical grating, 4-10 s cumulated exposition time were used. The spectral resolution of measurements was 3.0 cm^{-1}. The step size of the Raman maps varied between 1 and 0.5 µm for magnifications 50× and 100×, respectively. Representative Raman maps and their spectra are shown in Figure 4.

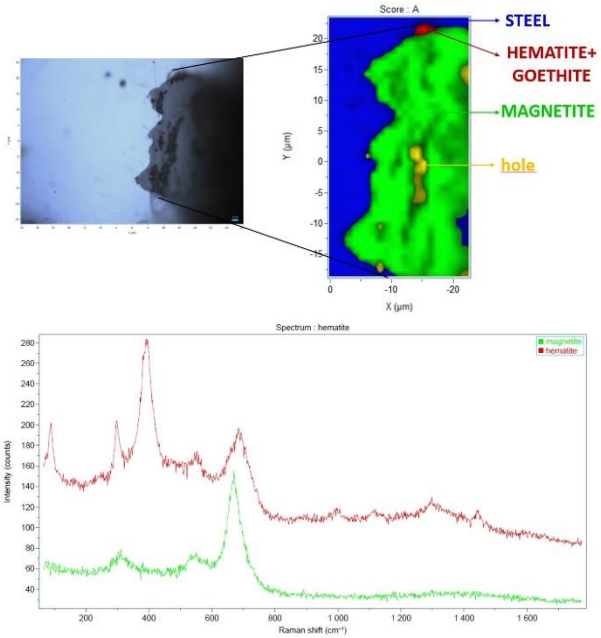

Fig. 4a. µRaman map and characteristic spectra obtained for C-steel-clay system after 3 months.

Mainly magnetite (Fe_3O_4) and hematite (α-Fe_2O_3)-goethite (α-FeO(OH)) can be identified on the SC-3M sample (Fig. 4a). Formation of Fe_3O_4 confirms the anoxic corrosion of the carbon steel under anaerobic conditions [1]. All iron-oxides present a main peak in the region of 600-700 cm^{-1}, except in the case of hematite and goethite [7].

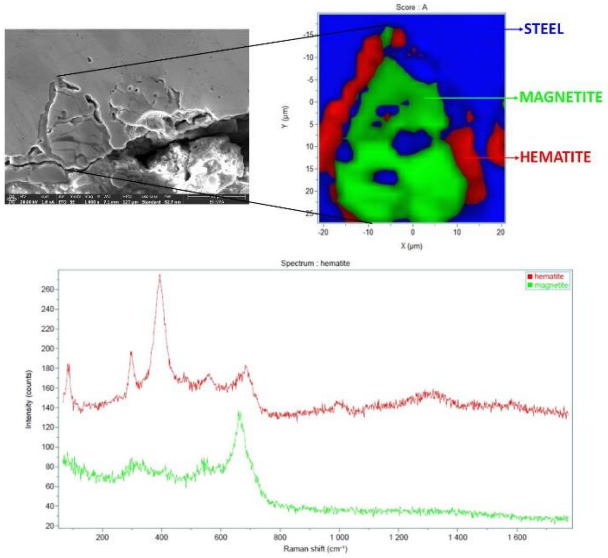

Fig. 4b. µRaman map and characteristic spectra obtained for C-steel-clay system after 7 months.

Hematite (α-Fe_2O_3) and magnetite (Fe_3O_4) can be identified as corrosion products after 7 months (Fig. 4b.). The corrosion protrusion is formed by magnetite, which is surrounded by hematite. No other corrosion products could be identified by the methods used. In clay environments, the carbon steel surface is likely to be passive due to the formation of a stable Fe_3O_4 film, and will persist under anaerobic conditions, ensuring passivity until degradation of the clay barrier.

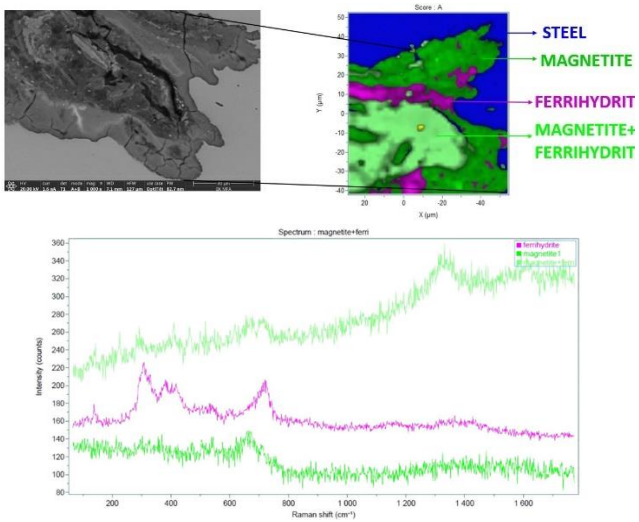

Fig. 4c. µRaman map and characteristic spectra obtained for C-steel-clay system after 12 months.

After 12 months of experiments substantial changes in the Raman spectra were observed (Fig. 4c). Magnetite (Fe_3O_4) and ferrihydrite ($Fe_{10}O_4(OH)_2$) were detected. Ferrihydrite has been shown to form in atmospheric corrosion conditions [1], which suggest that at last stage of the experiments, 12M

the initial anaerobic conditions became partly aerobic. The anaerobic conditions may coexist with aerobic ones: oxygen in gaseous form could be present in the macro-environment (water). The occurrence of an aerobic SBPW and anaerobic clay systems can be defined as anaerobic, saturated aqueous phase. The chemistry of the SBPW could evolve over time. The primary corrosion product of anaerobic C-steel corrosion is widely accepted to be $Fe(OH)_2$, however, is not considered to be thermodynamically stable under anaerobic conditions generally transforms to Fe_3O_4. The high temperature also favors the formation of Fe_3O_4, which was detected after 3M, 7M and found after 12M. In presence of O_2 (a slightly oxidizing condition could appear, thanks to the dissolution of O_2 from SBPW) [8], Fe^{III} oxides/oxyhydroxides become the corrosion product species. FeOOH corrosion products formed on the steel container due to the presence of trace levels of O_2 (after 12M the ferrihydrite was detected). The conditions could become progressively more aerobic with time. Carbon steel corrosion in simulated geological conditions (clay, SBPW) results in a variety of corrosion products of varying proportions with exposure time. During the exposure time magnetite was identified as the main corrosion product while at longer times (12M) ferrihydrite is formed. These structural modifications are due to changes of conditions with time exposure. No iron-carbonates or iron-sulfides were identified.

III.4. Analysis of leaching into porewater

We were able to collect sample from the liquid phase surrounding the inner Teflon container of which inductively coupled plasma - optical emission spectrometry (ICP-OES) and ion chromatography (IC) investigations were performed after 3, 7 and 12 months.

ICP-OES measurements were carried out on a Perkin Elmer Avio 200 sequential instrument. All elements were tested in radial view using Y as internal standard. The leachates were filtered through a cellulose acetate membrane (dp > 220 nm) and then were acidified with 2 m/m% nitric acid. The power of the generator was set to 1200 W during the measurements and the use of plasma argon was 12 l/min. IC analyses were performed on a Thermo Scientific Dionex Aquion equipment. B, Ca, K, Mg, Na and Si concentrations were determined using ICP-OES (Table IV), while IC was used for Cl^- and SO_4^{2-} (Table V).

Higher K, B and Na concentration was found in the final porewater of the CSC-7M and CSC-12M systems compared to the initial conditioned porewater. Elevated K and B concentrations from baseline can be traced back to clay content, having initially 4.7 wt.% K_2O and 200-300 mg/kg B [9]. The concentration of K jumped one order of magnitude. Concentration of bivalent cations (Ca and Mg) did not change significantly. Higher Si concentration was measured after 7 months but showed a decrease afterwards. The dissolution of Ca, K and Na increased after 7 months.

	B	**Ca**	**K**	**Mg**	**Na**	**Si**
[mg/l]						
SBPW recipe	-	125	7	57	380	-
SBPW conditioned	0.12	108	22	49	492	5.9
CSC-7M	1.7	100	48.3	55.1	454	34.9
CSC-12M	4.6	106	134	50.2	534	31.4

TABLE IV. ICP-OES results, comparing the 7-12 months sampling

IC analysis of the liquid phase shows that chloride concentrations remained near the concentration of the porewater. In contrast, the dissolved concentration of sulfate increased to 7M, after that, to 12 M became constant. The increase was less than 10% for chloride but higher for sulfate.

	Cl^-	**SO_4^{2-}**
[mg/l]		
SBPW recipe	817	182
SBPW conditioned	823	183
CSC-3M	819.1	193.7
CSC-7M	819.6	221.7
CSC-12M	831.1	221

TABLE V. IC results, comparing the 3-7-12 months sampling

DISCUSSION

Several studies focus on understanding of corrosion activity on the clay-rich formation under DGR conditions or predicted conditions [10-14]. The Hungarian radioactive waste management company (PURAM) is designing a DGR in Boda Claystone Formation (BCF) in West-Mecsek (SW-Hungary). To date there has been no corrosion investigations for the BCF, therefore the present investigations were conducted to optimize and finalize this repository concept with the aim to ensure its long-term safety.

The corrosion experiment lasted for one year. During the experiment the temperature was controlled, the corrosion potential was monitored. Corrosion potential fluctuation can be detected for the samples in the course of the experiment, except for the CSC-M12 sample where the corrosion potential reached a nearly constant value after six months. To exclude leakage and ensure saturation, the mass of each experimental setup was inspected monthly.

Microstructural characterization shows that all three C-steel containers corroded in BCF. The corrosion interfaces bear some similarities in the behavior of 3-, 7- and 12-months samples. The 3- and 7-months samples contain magnetite and hematite, with low Cl activity, but significant sulfate

movement that is notable in the porewater composition. The amount of Fe(III)- and Fe(II)-oxide phases are remarkable, but other Fe-based phases (e.g. Fe-silicate, Fe-sulfide) are absent. The presence of significant amounts of Fe-hydroxide for CSC-M12, clearly indicates oxic conditions, however, the exact timing of this interaction remains uncertain, predicted between 7M and 12M. Higher amount of Cl can be found in the CSC-12M solution, indicating a higher dissolution than for 3M and 7M samples. Sulfate dissolution remain at the same level as in 7M sample.

Based on the SEM/μRaman results for the CSC-3M and CSC-7M samples the presence of corrosion layer can be identified, the main corrosion product containing magnetite and hematite. These results are strongly analogous with similar experiments conducted under anaerobic conditions [15,16].

IV. CONCLUTIONS

Carbon steel corrosion in simulated geological conditions (BCF, porewater, 80°C) results in a variety of corrosion products of varying proportions with exposure time. At short time (3M and 7M) exposure magnetite and hematite was identified as the main corrosion product, while at longer time (12M) magnetite and ferrihydrite are formed. These microstructural modifications are due to changes of conditions from anoxic to oxic with time including chloride and sulfate activity. As expected from the literature, non-uniform general corrosion has been identified and the different corrosion products as well as their chronological order of formation have been highlighted.

The present work shows that it is important to consider all the components of a disposal site to explain the corrosion mechanism and need to conclude that the present timeframe was not sufficient to understand all corrosion mechanisms which could take place in the investigated systems.

ACKNOWLEDGMENTS

The research was supported by the European Joint Programme on Radioactive Waste Management (EURAD) Assessment of chemical evolution of ILW and HLW disposal cell (ACED) work package (EU grant agreement number: 847593). One of the authors (M.F.) acknowledge that this project was party supported by the János Bolyai Research Scholarship of the Hungarian Academy of Sciences.

REFERENCES

1. L. W. HILL SHANNON, Electronic Thesis and Dissertation Rep. The University of Western Ontario, Graduate program in Chemistry (2016).
2. J.-M. GRAS, *C.R. Physique*, **3**, 891 (2002).
3. D. CRUSSET, V. DEYDIER, S. NECIB, J-M. GRAS, P. COMBRADE, D. FERON and E. BURGER, *Corr. Eng. Sci. and Tech.*, **52**, 17 (2017).
4. K. LAZAR and Z. MATHE, Chapter 4., Ed. Dr. Marta Valaskova, University of Ostrava, ISBN: 978-953-51-0738-5, InTech (2012).
5. D. BREITNER, J. OSAN, M. FABIAN, P. ZAGYVAI, CS. SZABO, R. DAHN, M. M. FERNANDES, I. E. SAJO, Z. MATHE and SZ. TOROK, *Environ. Earth Sci.*, **73(1)**, 209 (2014).
5. F. KING, Corrosion of Carbon Steel, AMEC Rep. Ref. 17697-TR-03 Appendix B.2, Nuclear Decommissioning Authority (2014).
6. N. BOUCHERIT, A. H. L. GOFF and S. JOIRET, *Corr. Sci.*, **32**, 497 (1991).
7. M. L. SCHLEGEL, C. BATAILLON, C. BLANC, D. PRET and E. FOY, *Env. Sci. & Tech.*, **44**, 1503 (2010).
8. L. ARRIBA-RODRIGUEZ, J. VILLANUEVA-BALSERA, F. ORTEGA-FERNANDEZ and F. RODRIGUEZ-PEREZ, *Metals*, **8**, 334 (2018).
9. E. TOTH, E. HRABOVSZKI, T.M. TOTH and F. SCHUBERT, *J. Struct. Geol.*, **138**, 104105 (2020).
10. T. BEHRENDS and C. BRUGGEMAN, OPERA-PU-UTR611-1, Utrecht University, SCK·CEN (2016).
11. Y. EL. MENDILI, A. ABDELOUAS, A. A. CHAOU, J.-F. BARDEAU and M. L. SCHLEGEL, *Corr. Sci.*, **88**, 56 (2014).
12. M. L. SCHLEGEL, F. MARTIN, M. FENART, C. BLANC, J. VARLET and E. FOY, *Corr. Sci.*, **184**, 109368 (2021).
13. S. NECIB, N. DIOMIDIS, P. KEECH and M. NAKAYAMA, *Swiss J. Geosci.*, **110**, 329 (2017).
14. N. R. SMART, B. REDDY, A. P. RANCE, D. J. NIXON, M. FRUTSCHI, R. BERNIER.LATMANI and N. DIOMIDIS, *Corr. Eng. Sci. Tech.*, **52**, 101 (2017).
15. M. L. SCHLEGEL, C. BATAILLON, K. BENHAMIDA, C. BLANC, D. MENUT and J.-L. LACOUR, *Appl. Geochem.*, **23**, 2619 (2008).
16. H. EL HAJJ, A. ABDELOUAS, Y. EL MENDILI, G. KARAKURT, B. GRAMBOW and C. MARTIN, *Corr. Sci.*, **76**, 432 (2013).